The published version of the paper "Morbidelli R., Saltalippi C., Flammini A., Cifrodelli M., Picciafuoco T., Corradini C., Govindaraju R.S. (2016). Laboratory investigation on the role of slope on infiltration over grassy soils. Journal of Hydrology, 543, 542-547." is available at: https://doi.org/10.1016/j.jhydrol.2016.10.024

Laboratory investigation on the role of slope on infiltration over grassy soils

Renato Morbidelli, Carla Saltalippi, Alessia Flammini, Marco Cifrodelli, Tommaso Picciafuoco, Corrado Corradini

Dept. of Civil and Environmental Engineering, University of Perugia, via G. Duranti 93, 06125 Perugia, Italy

Rao S. Govindaraju

School of Civil Engineering, Purdue University, West Lafayette, IN 47907

Abstract

Even though natural surfaces are rarely horizontal, infiltration modeling has been primarily confined to horizontal surfaces, and there are not enough studies to clarify the effects of slope on the partition of rainfall into surface and subsurface water. Besides, previous experimental results on the effects of slope provide conflicting conclusions perhaps because of the existence of erosion and crust formation. In this study,new laboratory experiments, performed in the absence of the last two processes, highlight the effect of the slope angle, γ, on infiltration into a grassy soil. The results are compared with those from previous experiments performed on a bare soil and interpreted in terms of an effective soil saturated hydraulic conductivity, K_e (γ). The grassy soil dampens the variation of K_e with γ compared to bare soil. For example, for γ=10°, the reduction of the gravitational infiltration with respect to the saturation condition was ~ 80% for the bare soil, while we find it to be ~ 20 % for the grassy soil. Finally, we point out that the presence of grass does not affect the results through the development of a two layered soil, but through a substantial variation of roughness.

Key words: Hillslope hydrology, Infiltration experiments, Infiltration modeling, Surface runoff.

1. Introduction

Rainfall infiltration influences surface runoff production from the local (point) to field scale, playing a significant role in the hydrological responses of hillslopes and watersheds as well as in the generation of water flow and transport of pollutants in subsurface layers. It is widely recognized that the process is mainly governed by rainfall rate, r, soil hydraulic properties and antecedent soil moisture content, θ_i, while the role of soil slope has not been fully understood. At the local scale many infiltration models have been proposed for regular storms and immediate ponding. The approach formulated by Green-Ampt (1911) extended for applications involving pre-ponding and post-ponding conditions (Mein and Larson, 1973; Chu, 1978), the extended Philip equation (Philip, 1969; Chow et al., 1988) and the Smith and Parlange approach (1978) then reformulated by Parlange et al. (1982) are examples of widely-used models. A simplified technique based on the time compression approximation was also proposed to extend the application of these approaches to complex rainfall patterns (Mls, 1980; Péschke and Kutílek, 1982; Verma, 1982). More comprehensive formulations were presented by Dagan and Bresler (1983) and later by Corradini et al. (1997) who realized a model describing successive infiltration-redistribution cycles determined by any erratic rainfall.

Some models representing infiltration at the field scale have been more recently proposed for saturated hydraulic conductivity, K_s, assumed as a random variable at the soil surface and homogeneous (Smith and Goodrich, 2000; Govindaraju et al., 2001) or not homogeneous (Corradini et al., 2011; Govindaraju et al., 2012) in the vertical direction. Further, models were developed to describe the effects of a joint horizontal variability of K_s and r (Wood et al., 1986; Castelli, 1996; Govindaraju et al., 2006; Morbidelli et al., 2006), and of the spatial variability of θ_i (Smith and Goodrich, 2000). The role of the heterogeneity of θ_i combined with uniform values of K_s and r or with K_s randomly variable has been widely analyzed for different spatial scales (Brontsert and Bardossy, 1999; Morbidelli et al., 2012; Hu et al., 2015).

In most real situations, infiltration occurs over sloping surfaces, while all the aforementioned models were developed for horizontal surfaces. Therefore, they need to be properly adapted for applications where surface slope has a significant influence on the partitioning of rainfall into surface and subsurface flow. This is still an open issue because of the limited and inconclusive results obtained from both theoretical and experimental investigations.

Poesen (1984), through laboratory experiments, observed that infiltration increased in steeper slopes for heavy rainfall rates and attributed this result to the processes of surface crust formation, more pronounced in flatter slopes, or rill erosion, that occurs more quickly on steeper slopes. This interpretation was also supported by the fact that for light rainfall events, infiltration was found to be unaffected by variations in the slope angle, γ. Chen and Young (2006) adapted the Green-Ampt approach for applications to sloping surfaces under the condition of identical slope horizontal projection lengths used to have equivalent rainfall input to different slope cases. They obtained an increase of infiltration with γ that could be neglected for $\gamma<10°$.

However, from previous field studies, Nassif and Wilson (1975) and Sharma et al. (1983) deduced a decrease of infiltration with increasing slope angle. A similar trend was obtained on the basis of laboratory experiments by Fox et al. (1997), who examined the infiltration process in an interril area with a vertical soil profile characterized by a thin sealing layer at the soil surface. Their results also indicated that the crust permeability was independent of the slope. Furthermore, a negative relationship between infiltration rate and γ was proposed by Philip (1991) through a mathematical approach. It involves a reduction of the gravitational effect on the infiltration rate by a factor of cos γ, which implies a decrease of 13% from γ=0° to γ=30°.

Essig et al. (2009) and Morbidelli et al. (2015) reported results from controlled laboratory experiments under conditions of dominant gravitational effects using bare soils. In the absence of sealing and erosion of top soil, they showed that infiltration decreased with increasing γ and overland flow was generated even for $r < K_s$. The observed trends agreed with those showed by Sharma et al. (1983) and Philip (1991), but the magnitudes of the reduction in infiltration with slope were much larger than expected from the earlier studies. Furthermore, Essig et al. (2009) and Morbidelli et al. (2015) examined the possibility of representing the infiltration process through an effective saturated hydraulic conductivity depending on soil roughness and to be used in the models set up for γ=0°.

The main objective of this paper is to address this last issue by providing experimental evidence on the role of roughness in the determination of the relation between infiltration and slope angle. In this context new laboratory experiments involving infiltration into a grassy soil have been performed, and a comparison of the results with those obtained earlier on bare soils using a similar experimental apparatus is provided.

2. Laboratory experimental system

The basic element used for the experiments is a physical model (Fig. 1) consisting of a soil tank 152 cm long, 122 cm wide and 78 cm deep with impermeable sides and slope angle that can vary in the range 1°-15° (1.8%-26.8%).

A natural soil with vertically uniform grain size distribution corresponding to loam soil according to the USDA classification was selected. It was carefully packed to a thickness of

67 cm and was placed on a gravel layer 7 cm deep to speed the drainage process. Furthermore, a natural grassy soil (see Fig. 1b) was realized with the aid of a lamp producing artificial radiation characterized by a wavelength spectrum similar to that of solar radiation. Artificial rainfall of almost uniform intensity was produced by pressurized water sprinklers. The characteristics of the rainfall fields were checked before the beginning of each experiment by a grid of pans placed on a metal sheet. Rainfall rates fairly different from the soil saturated hydraulic conductivity and well representative of many real situations were produced, considering also the importance to obtain infiltration results for r significantly larger than K_s as well as for r comparable to K_s.

The moisture content, θ, was monitored by a Time Domain Reflectometer (TDR) sensor used with a vertically oriented probe that provided continuous average measurements associated with the uppermost part of the soil (0-20 cm deep).

Continuous measurements of surface runoff and deep flow were carried out by tipping bucket sensors through triangular metal collectors, both placed at the outlet of the physical model. This solution to measure surface runoff was adopted considering that a comparison of the results earlier obtained by Essig et al. (2009) and Morbidelli et al. (2015) for bare soils indicated that the downstream boundary of the physical model did not influence significantly the partitioning of rainfall into surface and subsurface flow. More specifically, the trend of the infiltration observed in bare soils as a function of γ when the surface flow collector was placed at the lower tank side (Essig et al., 2009) or 50 cm upstream (Morbidelli et al., 2015) was identical.

3. Experiments and analysis of results

Many experiments were carried out for different γ and r values that varied in the range 1°-15° and 7-30 mmh^{-1}, respectively. The whole soil surface was subject to uniform rainfall of 8 h-duration, while surface and deep flow were continuously measured up to 14 h. Twenty-eight experiments were performed, each starting from a soil moisture vertical profile close to saturation. This condition was reached by application of a long duration rainfall before the beginning of each experiment. The grassy soil allowed us to set-up experiments with tank angles greater than 10°, which was the maximum angle for the experiments with bare soils carried out by Morbidelli et al. (2015) without causing surficial landslides. In each experiment, the long duration of steady rainfall generated surface (if any), and deep steady flows. The discharges observed at this stage represent the primary quantities for the analysis of the slope effects on infiltration and surface flow production.

Table 1 summarizes the steady flows obtained for different values of γ and r. We note that different equipment was used in the artificial rainfall generation. Most experiments were performed using the same sprinkler, while those with water pressure denoted by 1.0^ bar and 1.0* bar were realized using one larger sprinkler and two sprinklers, respectively. As it can be seen, the rainfall rates associated with a given value of water pressure and the same sprinklers characteristics are not the same in the four experiments performed for γ=1°, 5°, 10° and 15°, however the variability in r is less than 10%. These differences were due to the fact that no more than one experiment per day could be carried out and the pressurized water sprinkler system was turned off and switched on for the successive experiment. This procedure, coupled with the limited resolution in the selection of water pressure, did not allow us to exactly obtain a fixed value of r. We chose the lowest value of γ equal to 1° because it was the minimum value that enabled us to carry out accurate measurements of flow. The deep flow observed for γ=1° should be representative of the infiltration process into a horizontal soil surface.

An analysis of the data of Table 1 for γ=1° allows us to identify the deep flow observed under the rainfall rate of 29.9 mmh^{-1} as the soil saturated hydraulic conductivity (i.e. K_s=28.7 mmh^{-}

^{1}) because the production of surface runoff indicates surface saturation. The achievement of steady conditions, with equality in the sum of surface and deep flow rates with the rainfall rate, indicates that the soil moisture vertical profile is uniform and time invariant with water content equal to the saturation value, θ_s. These deductions are confirmed by the results shown in Fig. 2 for the same experiment, where it can be observed a long steady state for both surface and deep flow together with a corresponding steady condition for the soil moisture content.

Similar reasoning can be extended to the other experiments performed with γ=1°-15° that did not produce surface runoff. In particular, during the period with steady deep flow a steady water content was also observed in these experiments, and the soil water vertical profile was uniform with value of θ ($<\theta_s$) that decreased with the steady rainfall rate.

The main results shown in Table 1 are associated with the maximum value of r used for each slope angle. Further results of these experiments are illustrated in Figs. 3 and 4 through the comparison of the deep flow hydrographs and that of surface and deep flow for the representative experiment with γ=5°, respectively. As seen in Fig. 3, the duration of the steady stage is very long (~ 6 h) - practically independent of γ – as is the surface flow. In addition, Fig. 4 highlights that the steady stage of the surface runoff precedes that of the deep flow by nearly 1 h. From these results, we deduce that when surface runoff starts, the surface water content has reached the maximum possible value for a given γ value and that in the time interval between the beginning of the two steady conditions being attained, the vertical θ profile becomes uniform. Therefore, for each slope angle the steady deep flow observed under the highest value of r can be considered to represent the maximum value that can be reached by the soil hydraulic conductivity, henceforth denoted as effective saturated hydraulic conductivity $K_e(\gamma)$. The K_e values decrease with increasing γ and range from $K_e(\gamma=1°)\approx K_s=28.7$ mmh^{-1} to $K_e(\gamma=15°)=21.4$ mmh^{-1}. This variation is more pronounced than that expected if the Philip (1991) representation of the gravitational effect, $K_e(\gamma)=K_s\cos\gamma$, was applied. In fact the last formulation would produce $K_e(\gamma=15°)=27.8$ mmh^{-1} that is very close to the hydraulic conductivity value associated with a nearly horizontal soil surface. An important effect due to the existence of $K_e(\gamma)<K_s$ is the generation of surface runoff for $K_e(\gamma)<r<K_s$ as shown for example in Tab.1 where for $\gamma=10°$ we have surface flow with r=28.0 mmh^{-1}, $K_e=22.8$ mmh^{-1}, and for $\gamma=15°$ with r=27.7 mmh^{-1}, $K_e=21.4$ mmh^{-1} while $K_s=28.7$ mmh^{-1}.

The trend observed in the above-discussed trials for a grassy soil, in the absence of capillary contributions, is similar to that earlier obtained by Morbidelli et al. (2015) for a bare soil, however the magnitude of the slope effect on the infiltration process is significantly less. Figure 5 highlights these changes by using the measurements earlier carried out in a bare soil with $K_s=8.15$ mmh^{-1} subjected to the maximum rainfall rate for $\gamma=5°$ and 10° (r=11.6 mmh^{-1} and 11.7 mmh^{-1}, respectively). The comparison does not include the case with $\gamma=15°$ because of surface landslide formation in the bare soil. The decrease of the infiltration rate in the grassy soil is limited to 20%, while in the bare soil it reaches values of about 40% and 80% for $\gamma=5°$ and 10°, respectively.

We note that for each γ value the corresponding K_e has been assumed invariant with depth and equal to the steady deep flow observed for the value of r that produced a significant surface runoff. This approach is clearly correct for the experiments with the bare homogeneous soil, while the presence of grass in the homogeneous soil determines the formation of a two-layered soil with a greater permeability in the upper part (Morbidelli et al., 2014). An assessment of the effects of the vertical heterogeneity of hydraulic conductivity has been therefore performed using representative cases of infiltration into a horizontal soil. In particular two different soil profiles have been considered: (1) an underlying soil with $K_s=28.7$ mmh^{-1} and an upper layer 5 cm deep with a doubled value of K_s; (2) a homogeneous soil with K_s=28.7 mmh^{-1}. Simulations have been performed by the model formulated by Corradini et al. (2000) and earlier tested by comparison with numerical solutions of the Richards equation. The rainfall pattern previously used, with γ=1°, to derive the K_s value in the grassy soil has been applied. The simulations have shown that during the period with steady deep flow the infiltration rate was invariant from a soil profile to the other. This is due to the fact that in this stage the entire two-layered soil is saturated and the deep flow is governed by the underlying soil with smaller permeability. The same mechanisms can be expected to act in the other experiments with sloping surface. This analysis strengthens the interpretation of the results we have provided on the basis of K_s and $K_e(\gamma)$ independent of depth even in the grassy soil.

Finally, we specify that our pressurized water system did not enable us to realize additional trials with greater and spatially uniform rainfall rates. Experiments with r significantly larger than K_s could have provided a further support to our deductions on the maximum values of $K_e(\gamma)$. However, the trend of the steady deep flow observed in a bare soil by Morbidelli et al. (2015) for r considerably larger than K_s supports our interpretations.

4. Concluding remarks

In spite of the appreciable number of investigations set up to clarify the relationship between infiltration rate and slope gradient, the solution of this issue remains still undefined. Many field/laboratory experiments together with theoretical studies resulted in conflicting interpretations of the existing relationships. This was probably due to confounding effects of additional processes such as the formation of sealing layers and rills.

Our laboratory physical system allowed us to perform trials under conditions of dominant gravitational effects and in the absence of crust and erosion.

In two previous studies (Essig et al., 2009; Morbidelli et al., 2015) the influence of γ on infiltration rate and surface runoff generation for bare soils was showed through a combination of experimental results and numerical simulations.

The primary motivation of this experimental investigation was to further improve our understanding of the role of slopes on bare surfaces with respect to that on grassy surfaces. In this context, we provide evidence of the relationship between γ and infiltration rate on a grassy soil. Our experiments point out that the effect of slope gradient on infiltration rate is greatly reduced by the grassy soil surface through a smaller decrease of the steady infiltration rate for γ ranging from 1° to 15°. More specifically our results provide evidence of the existence of an effective soil saturated hydraulic conductivity $K_e(\gamma)$ associated with rainfall rates that produce surface runoff and steady deep flow for each γ value. This quantity decreases from ~K_s for γ=1° down to ~0.8 K_s for γ=10° while its decrease through the factor cosθ would be less than 2%. The mentioned discrepancy becomes much more important in the case of a bare soil for which, from Morbidelli et al. (2015), $K_e(\gamma=10°)\approx 0.2\ K_s$.

A common feature of slopes with grassy soils and bare soils concerns the generation of surface runoff also for $K_e<r<K_s$, that is in unsaturated soils. Furthermore: (1) the trials presented in this work for a grassy soil coupled with those earlier described for bare soils suggest that the magnitude of the effects of γ on the gravitational component of infiltration rate into a flat surface is determined by a mechanism independent of the formation of rills or a sealing layer. In fact they were not affected by the last two processes, which influenced several previous investigations; (2) the formation of a two-layered soil due to the grass growth cannot explain the effects of γ on the infiltration rate; and (3) the aforementioned mechanism is strictly dependent on the surface roughness.

Finally, we remark on a critical point of our investigation. Due to limitations of the available artificial rainfall generator, a different soil similar to that used by Morbidelli et al. (2015), with saturated hydraulic conductivity of 8.15 mmh^{-1}, would have allowed us to support our analysis with more experiments where $r>K_e(\gamma)$. However, in spite of starting from the same grain size distribution and following a similar procedure, we did not obtain a soil close to the desired K_s value.

Acknowledgment

This research was mainly financed by the Italian Ministry of Education, University and Research.

References

Bronstert, A., Bardossy, A., 1999. The role of spatial variability of soil moisture for modeling surface runoff generation at the small catchment scale. Hydrol. Earth Syst. Sc. 3, 505-516.

Castelli, F., 1996. A simplified stochastic model for infiltration into a heterogeneous soil forced by random precipitation. Adv. Water Resour. 19(3), 133-144.

Chen, L., Young, M.H., 2006. Green-Ampt Infiltration Model for Sloping Surfaces. Water Resour. Res. 42, W07420, doi: 10.1029/2005WR004468.

Chow, V.T., Maidment, D.R., Mays, L.W., 1988. Applied Hydrology, McGrow-Hill, New York.

Corradini, C., Melone, F., Smith, R.E., 1997. A unified model for infiltration and redistribution during complex rainfall patterns. J. Hydrol. 192, 104-124.

Corradini, C., Melone, F., Smith, R.E., 2000. Modeling local infiltration for a two layered soil under complex rainfall patterns. J. Hydrol. 237, 58-73.

Corradini, C., Flammini, A., Morbidelli, R., Govindaraju, R.S., 2011. A conceptual model for infiltration in two-layered soils with a more permeable upper layer: From local to field scale. J. Hydrol. 410, 62-72.

Dagan, G., Bresler, E., 1983. Unsaturated flow in spatially variable fields, 1, Derivation of models of infiltration and redistribution. Water Resour. Res. 19(2), 413-420.

Essig, E.T., Corradini C., Morbidelli, R., Govindaraju, R.S., 2009. Infiltration and deep flow over sloping surfaces: Comparison of numerical and experimental results. J. Hydrol. 374, 30-42.

Fox, D.M., Bryan, R.B., Price, A.G., 1997. The influence of slope angle on final infiltration rate for interrill conditions. Geoderma 80, 181-194.

Govindaraju, R.S., Corradini, C., Morbidelli, R., 2006. A semi-analytical model of expected areal-average infiltration under spatial heterogeneity of rainfall and soil saturated hydraulic conductivity. J. Hydrol. 316, 184-194.

Govindaraju, R.S., Morbidelli, R., Corradini, C., 2001. Areal infiltration modelling over soils with spatially correlated hydraulic conductivities. J. Hydrol. Eng. 6(2), 150-158.

Govindaraju, R. S., Corradini, C., Morbidelli, R., 2012. Local and field-scale infiltration into vertically non-uniform soils with spatially-variable surface hydraulic conductivities. Hydrol. Proc. 26 (21), 3293-3301.

Green, W.A., Ampt, G.A., 1911. Studies on soil physics: 1. The flow of air and water through soils. J. Agricol. Sci. 4, 1-24.

Hu, W., She, D., Shao, M., Chun, K.P., Si, B., 2015. Effects of initial soil water content and saturated hydraulic conductivity variability on small watershed runoff simulation using LISEM. Hydrol. Sci. J. 60(6), 1137-1154.

Mein, R.G., Larson, C.L., 1973. Modeling infiltration during a steady rain. Water Resour. Res. 9, 384-394.

Mls, J., 1980. Effective rainfall estimation. J. Hydrol. 45, 305-311.

Morbidelli, R., Corradini, C., Govindaraju, R.S., 2006. A field-scale infiltration model accounting for spatial heterogeneity of rainfall and soil saturated hydraulic conductivity. Hydrol. Proc. 20, 1465-1481.

Morbidelli, R., Corradini, C., Saltalippi, C., Brocca, L., 2012. Initial soil water content as input to field-scale infiltration and surface runoff models. Water Resour. Manag. 26, 1793-1807.

Morbidelli, R., Saltalippi, C., Flammini, A., Cifrodelli, M., Corradini, C., Govindaraju, R.S., 2015. Infiltration on sloping surfaces: Laboratory experimental evidence and implications for infiltration modelling. J. Hydrol. 523, 79-85.

Nassif, S., Wilson, E., 1975. The influence of slope and rain intensity on overland flow and infiltration. Hydrol. Sci. Bull. 20, 539-553.

Péschke, G., Kutílek, M., 1982. Infiltration model in simulated hydrographs. J. Hydrol. 56, 369-379.

Philip, J.R., 1969. Theory of infiltration. Adv. Hydrosci. 5, 215-216.

Philip, J.R., 1991. Hillslope Infiltration: Planar Slopes. Water Resour. Res. 27(1), 109-117

Poesen, J.,1984. The Influence of Slope Angle on Infiltration Rate and Hortonian Overland Flow Volume. Z. Geomorphol. 49, 117-131.

Sharma, K., Singh, H., Pareek, O., 1983. Rain water infiltration into a bar loamy sand. Hydrol. Sci. J. 28, 417-424.

Smith, R.E., Goodrich, D.C., 2000. A model to simulate rainfall excess patterns on randomly heterogeneous areas. J. Hydrol. Eng. 5(4), 355-362.

Smith, R.E., Parlange, J.-Y., 1978. A parameter-efficient hydrologic infiltration model. Water Resources Research 14, 533-538.

Verma, S.C., 1982. Modified Horton's infiltration equation. J. Hydrol. 58, 383-388.

Wood, E.F., Sivapalan, M., Beven, K., 1986. Scale effects in infiltration and runoff production. Proc. of the Symposium on Conjunctive Water Use, IAHS Publ. N. 156, Budapest.

List of Tables

Table 1

Steady flows observed in laboratory experiments with artificial rainfalls over sloping grassy soil surfaces. The symbols ^ and * denote a pressurized water system with a larger sprinkler and two different sprinklers, respectively.

Figure Captions

Fig. 1. Laboratory experimental system: (a) soil tank with adjustable slope angle with a TDR sensor for soil moisture content; (b) image of the grassy soil surface.

Fig. 2. Experimental hydrographs observed for a grassy soil surface with slope of 1° under a rainfall rate of 29.9 mmh^{-1} and duration 8 h. The average soil moisture content measured close to soil surface is also shown.

Fig. 3. Deep flow hydrographs observed under the maximum rainfall rate (see Table 1) of duration 8 h generated for each slope angle.

Fig. 4. Experimental hydrographs observed for a grassy soil surface with slope of 5° under a rainfall rate of 30.4 mmh^{-1} and duration 8 h.

Fig. 5. Ratio between steady deep flow and saturated hydraulic conductivity observed under the maximum rainfall rate generated for each slope angle. The quantities referred to the bare soil are taken from Morbidelli et al. (2015).

Table 1 - Steady flows observed in laboratory experiments with artificial rainfalls over sloping grassy soil surfaces. The symbols ^ and * denote a pressurized water system with a larger sprinkler and two different sprinklers, respectively.

Water pressure	**Average rainfall rate**	**Steady surface flow**		**Steady deep flow**	
(bar)	**(mm h^{-1})**	**(mm h^{-1})**	**(%)**	**(mm h^{-1})**	**(%)**
slope angle 1°					
0.5	7.7	0	0	7.7	100.0
0.7	9.7	0	0	9.7	100.0
0.8	11.8	0	0	11.8	100.0
0.9	12.2	0	0	12.2	100.0
1.0	13.2	0	0	13.2	100.0
1.0^	17.1	0	0	17.1	100.0
1.0*	29.9	1.2	4.0	28.7	96.0
slope angle 5°					
0.5	8.6	0	0	8.6	100.0
0.7	10.7	0	0	10.7	100.0
0.8	11.2	0	0	11.2	100.0
0.9	12.6	0	0	12.6	100.0
1.0	12.4	0	0	12.4	100.0
1.0^	17.8	0	0	17.8	100.0
1.0*	30.4	6.3	20.7	24.1	79.3
slope angle 10°					
0.5	9.4	0	0	9.4	100.0
0.7	11.7	0	0	11.7	100.0
0.8	13.0	0	0	13.0	100.0
0.9	13.6	0	0	13.6	100.0
1.0	14.0	0	0	14.0	100.0
1.0^	16.6	0	0	16.6	100.0
1.0*	28.0	5.2	18.5	22.8	81.5
slope angle 15°					
0.5	8.1	0	0	8.1	100.0
0.7	11.5	0	0	11.5	100.0
0.8	13.0	0	0	13.0	100.0
0.9	13.7	0	0	13.7	100.0
1.0	11.7	0	0	11.7	100.0
1.0^	15.5	0	0	15.5	100.0
1.0*	27.7	6.3	22.7	21.4	77.3

(a) (b)

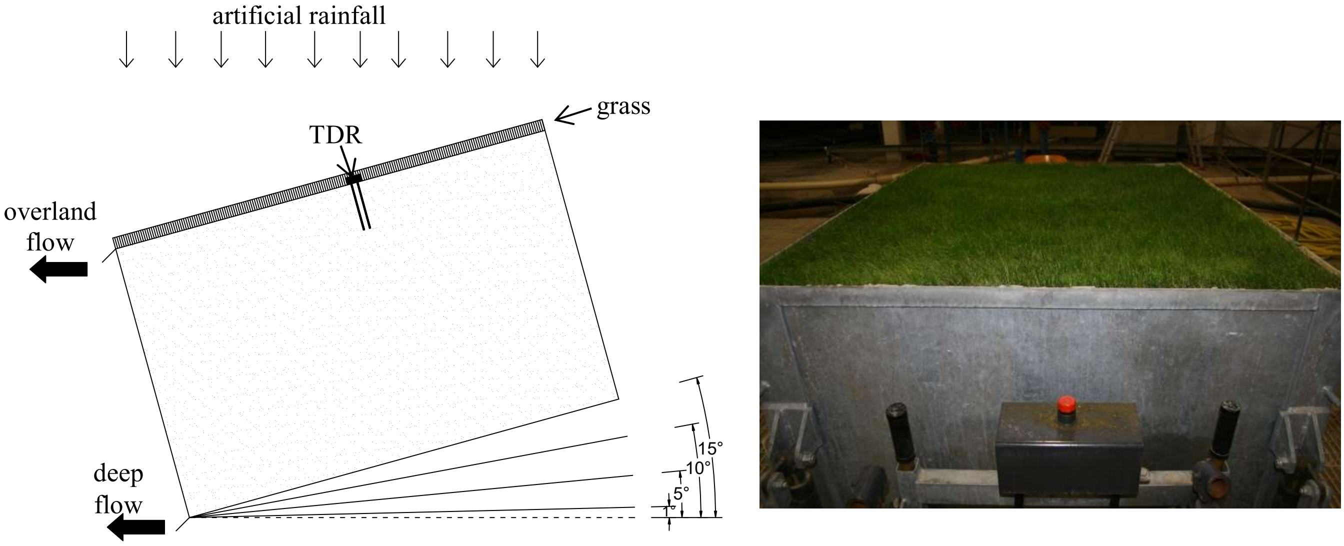

Fig. 1. Laboratory experimental system: (a) soil tank with adjustable slope angle with a TDR sensor for soil moisture content; (b) image of the grassy soil surface.

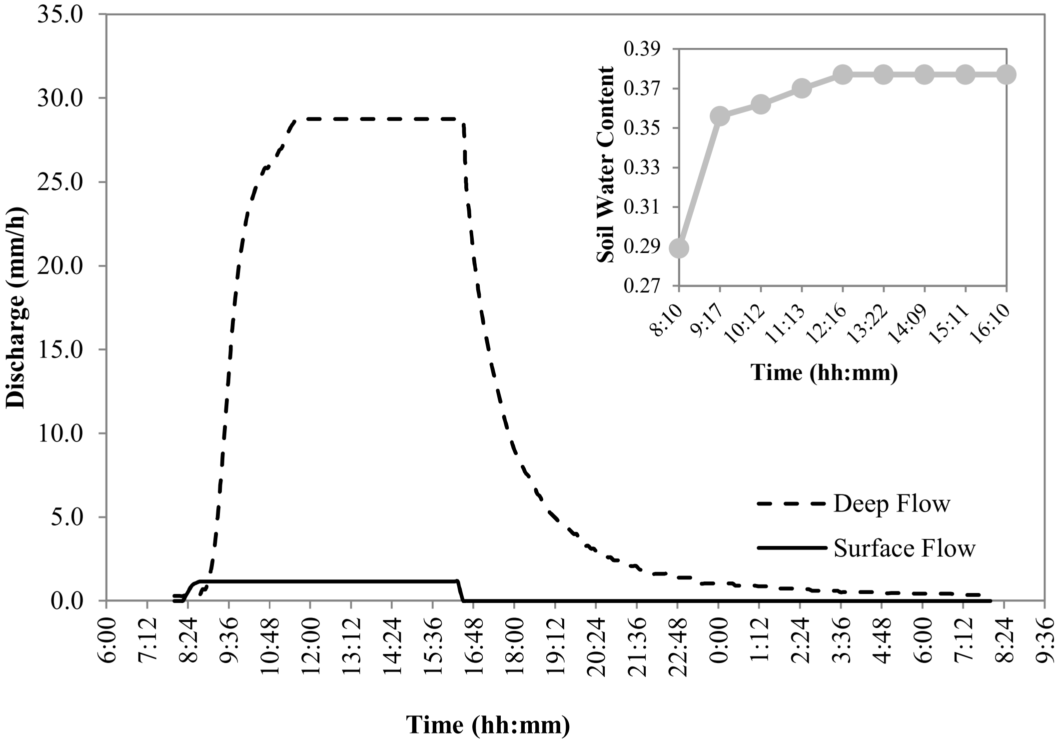

Fig. 2 - Experimental hydrographs observed for a grassy soil surface with slope of 1° under a rainfall rate of 29.9 mmh^{-1} and duration 8 h. The average soil moisture content measured close to soil surface is also shown.

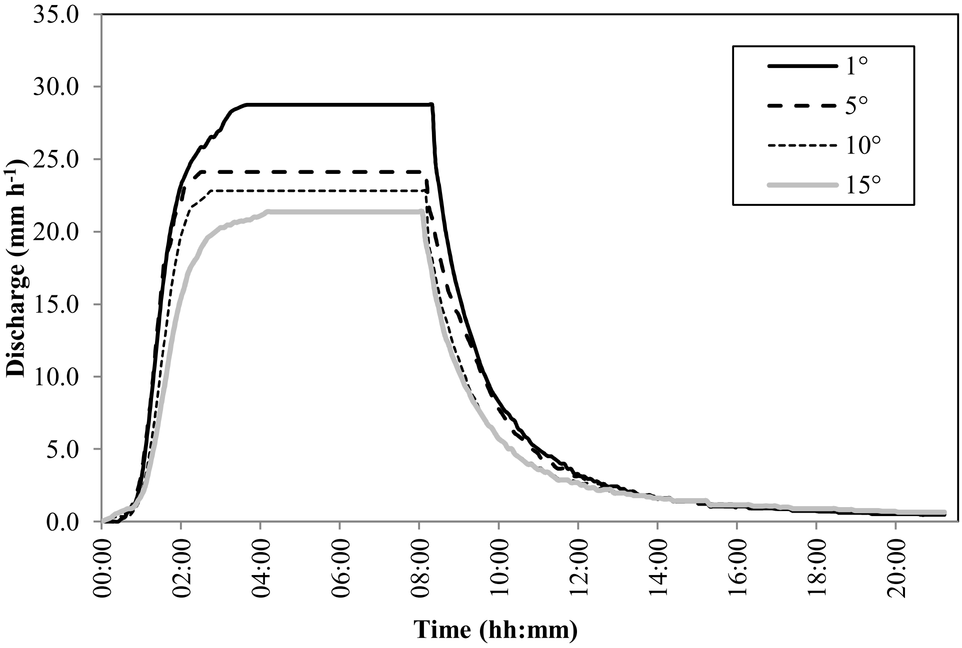

Fig. 3 - Deep flow hydrographs observed under the maximum rainfall (see Table 1) rate of duration 8 h generated for each slope angle.

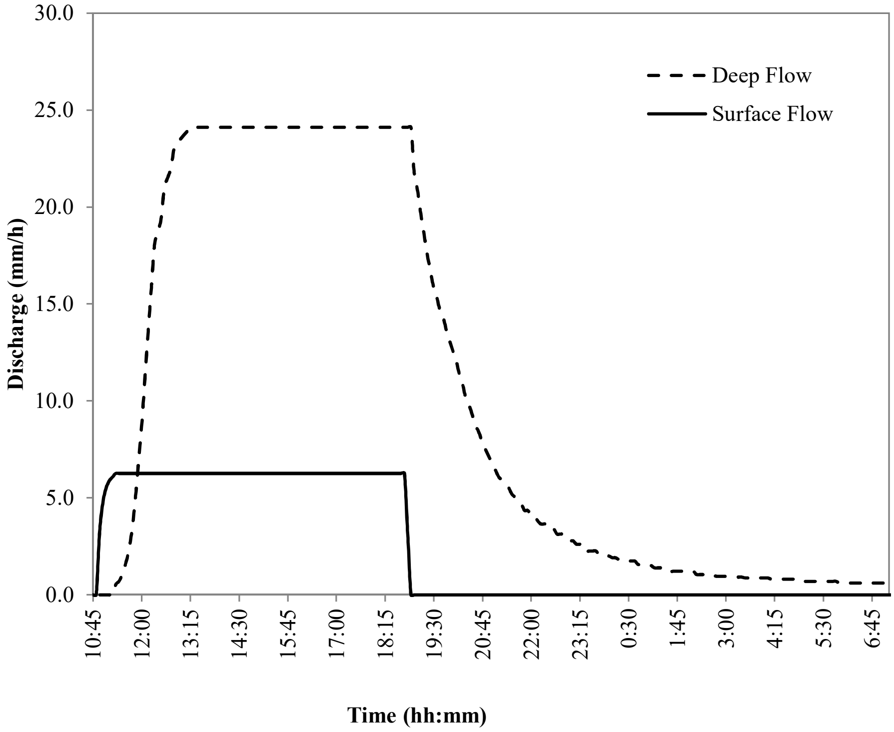

Fig. 4 - Experimental hydrographs observed for a grassy soil surface with slope of 5° under a rainfall rate of 30.4 mmh^{-1} and duration 8 h.

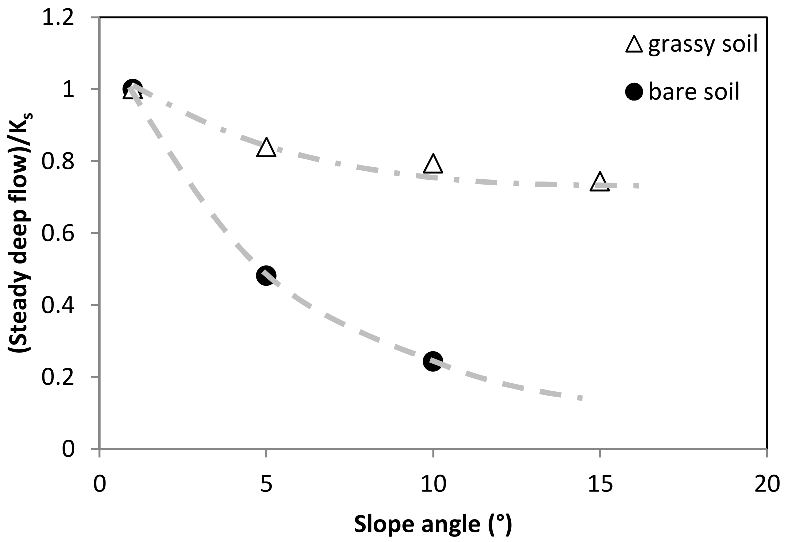

Fig. 5 - Ratio between steady deep flow and saturated hydraulic conductivity observed under the maximum rainfall rate generated for each slope angle. The quantities referred to the bare soil are taken from Morbidelli et al. (2015).